Correspondence

Modeling Nonlinear Wave Propagation on Nonuniform Grids Using a Mapped *k*-Space Pseudospectral Method

Bradley E. Treeby

***Abstract*—Simulating the propagation of nonlinear ultrasound waves is computationally difficult because of the dense grids needed to capture high-frequency harmonics. Here, a mapped *k*-space pseudospectral method is presented which allows the use of nonuniform grid spacings. This enables grid points to be clustered around steep regions of the wave field. Compared with using a uniform grid, this significantly reduces the total number of grid points needed for accurate simulations. Two methods for selecting a suitable nonuniform grid mapping are discussed.**

I. Introduction

The accurate and efficient numerical solution of nonlinear acoustic equations remains an important topic in biomedical ultrasonics and physical acoustics [1], [2]. However, simulating the propagation of nonlinear waves is a computationally difficult task because the medium discretization must be fine enough to capture harmonics that are generated as the ultrasound waves propagate. For strongly shocked waves, several hundred harmonics may be generated, resulting in the need for very dense computational grids [3]. This requirement is compounded if conventional finite-difference or finite-element methods are used to solve the governing equations, because large numbers of grid points per minimum wavelength are needed to avoid numerical dispersion [4]. To reduce this computational burden, several models for nonlinear ultrasound simulation based on the Fourier pseudospectral method have recently been presented [5]–[7]. These models use spectral methods to compute spatial gradients which allows discretizations close to the Nyquist limit of two grid points per minimum wavelength. Compared with finite-difference approaches, this can reduce the total number of grid points needed by as much as two orders of magnitude [6], [8]. However, a major limitation of current nonlinear ultrasound models based on the Fourier pseudospectral method is the restriction to uniform Cartesian grids. This means the discretization is globally constrained by the highest frequency of interest. That is, if two-points per wavelength are required to accurately represent the highest frequency harmonic somewhere in the domain, this grid spacing must be used everywhere. This penalty is of practical significance because the harmonic content produced by nonlinear waves does not usually exist uniformly over the domain. Here, we explore how this constraint might be overcome by using a mapped pseudospectral method to enable the use of nonuniform grid spacings. This allows the local discretization of the medium to be optimized to support the frequency content of the wave field in that region of the domain. Overall, this can yield a considerable saving in the total number of grid points (and thus memory and compute time) without compromising accuracy. The theory and background of the mapped pseudospectral method are given in Section II, with several numerical examples given in Section III. Discussion and summary are then given in Section IV.

Manuscript received January 21, 2013; accepted July 4, 2013. This work was conducted at the Research School of Engineering at the Australian National University, and supported by the Australian Research Council/Microsoft Linkage Project LP100100588.

The author is with the Department of Medical Physics and Bioengineering, University College London, London, UK (e-mail: b.treeby@ucl.ac.uk).

DOI http://dx.doi.org/10.1109/TUFFC.2013.2812

II. Theory

A. The Mapped Pseudospectral Method

The use of spectral methods to compute the gradient of discrete functions first gained popularity in the 1970s [9]. The general idea is to decompose the entire field into a finite sum of scaled basis functions that vary globally over the domain. The gradient can then be computed using the derivative of the basis functions. In the Fourier spectral method (which is the focus of this work), the basis functions are sinusoidal and the sampling points are evenly spaced. This allows the use of the fast Fourier transform (FFT) to compute the basis function weights. The advantage of this approach over finite-difference methods is that the grid spacing can often be much coarser for the same degree of accuracy [9]. In the context of modeling linear acoustic waves, this can be down to the Nyquist limit of two points per wavelength [8]. However, in nonlinear acoustics, the steepening waves generate high-frequency harmonics which also must be represented on the discrete computational grid.

The idea behind the mapped pseudospectral method is to discretize the field (in this case, the acoustic wave field) using a nonuniform grid such that any sharp or rapidly varying features are adequately resolved [9]. Given a mapping between the nonuniform grid x_n and a uniform grid with the same number of grid points x_u, spatial gradients can then be computed using the chain rule, where

$$\frac{\partial}{\partial x_\mathrm{n}} f = \frac{\mathrm{d}x_\mathrm{u}}{\mathrm{d}x_\mathrm{n}} \frac{\partial}{\partial x_\mathrm{u}} f = \frac{\mathrm{d}x_\mathrm{u}}{\mathrm{d}x_\mathrm{n}} \mathbb{F}_x^{-1}\{ik_x \mathbb{F}_x\{f\}\}. \qquad (1)$$

Here, the derivative with respect to the uniform grid points $\partial/\partial x_\mathrm{u}$ is calculated using the Fourier collocation spectral method without modification, where $\mathbb{F}$ represents the spatial Fourier transform, i is the imaginary unit, and k_x is the set of acoustic wavenumbers supported by the uniform grid.

The role of the mapping can be understood by imagining the nonuniform grid stretched out so the grid points are evenly spaced. In the transformed coordinates, regions in which the input function varies rapidly are much smoother. This allows the gradient to be computed more accurately. A simple example is shown in Fig. 1(b). Here, the solid line illustrates the original function sampled on a uniform grid. The dashed line shows the same function sampled using a nonuniform grid which is then stretched so the grid points are evenly spaced. Because the remapped function is smoother (meaning the Fourier coefficients decay more rapidly), the spectral gradient calculation is more accurate. The transformation gradient $\mathrm{d}x_\mathrm{u}/\mathrm{d}x_\mathrm{n}$ then maps the calculated gradient back to the original nonuniform grid points. For a given coordinate transform, the function $\mathrm{d}x_\mathrm{u}/\mathrm{d}x_\mathrm{n}$ can be precalculated and then applied each time the gradient is computed. This means the computational efficiency of the gradient calculation compared with the uniform case is largely preserved. Note, the transformation between x_u and x_n must have at least C^1 continuity (i.e., the transformation gradient must be continuous) [10].

An illustrative example of using a nonuniform grid to compute the gradient of a periodic function is shown in Fig. 1 (in this case, the function is chosen to be a one-dimensional cnoidal wave with an elliptic parameter of 0.99999). The nonuniform grid is defined by a periodic arctan/tan function [11], [12], where $x_\mathrm{n} = \arctan(a \tan x_\mathrm{u})$ for $x_\mathrm{u} \in [-\pi/2, \pi/2]$. The parameter $a \in [0, 1]$ controls the strength of the grid point clustering about $x = 0$. The crosses and dots in Figs. 1(a) and 1(b) show the function values sampled at uniform and nonuniform grid points, respectively, where $a = 0.5$ and $N_x = 12$ (here, N_x is the number of grid points). Fig. 1(c) illustrates the corresponding L_∞ error norm in the gradient calculation against the number of grid points N_x for simulations on both uniform and nonuniform grids (where $L_\infty = \max\{|f_\mathrm{ref}(x_i) - f_\mathrm{calc}(x_i)|: i = 1, 2, \ldots, N_x\}$). The error is noticeably reduced when the nonuniform grid mapping is used, with less than half the number of grid points required to reach machine precision. The variation in error with the clustering parameter a for $N_x = 50$ is shown in Fig. 1(d). For this example, the optimum value is around $a = 0.5$. However, the exact selection of this parameter is not critical, and there is a reduction in the error compared with the uniform case (shown with a dashed line) for a wide range of values.

The use of coordinate transformations to improve the accuracy of spectral methods in this fashion is not a new idea. In both electromagnetics and linear acoustics, the mapped pseudospectral method has previously been used to increase the density of grid points near known discontinuities in the medium properties [10], [13]. This can increase the accuracy of modeled transmission and

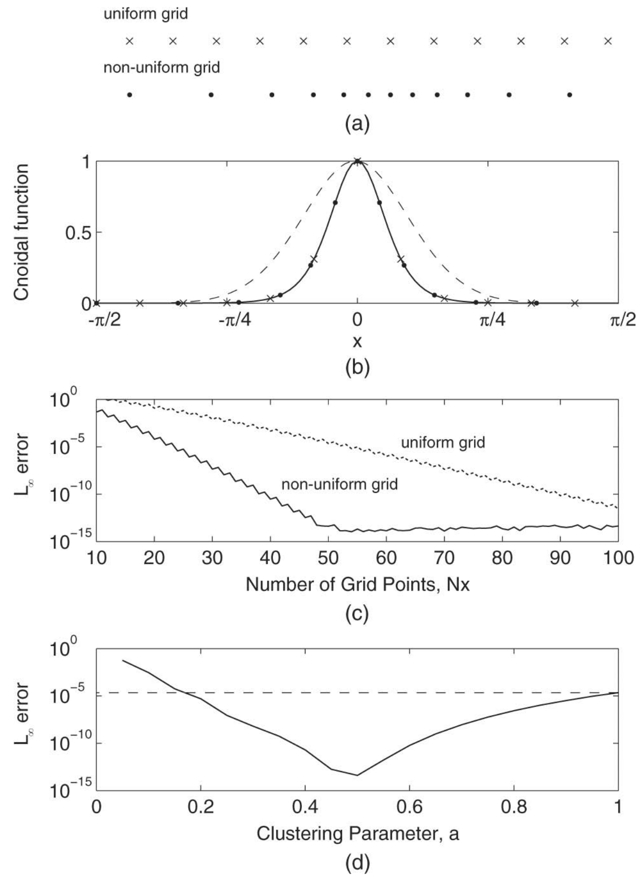

Fig. 1. Example of using a nonuniform grid mapping to compute the gradient of a periodic function. (a) Periodic uniform and nonuniform grid spacings created using an arctan/tan mapping with $N_x = 12$ and $a = 0.5$. (b) Periodic cnoidal wave (solid line) sampled using uniform (crosses) and nonuniform (dots) grids. The dashed line shows the nonuniform grid values stretched out so the grid points are evenly spaced. (c) Variation in the L_∞ error norm with the number of grid points for gradient calculations using uniform and nonuniform grid spacings. (d) Effect of the nonuniform clustering parameter a on the L_∞ error norm for $N_x = 50$. The corresponding error for the uniform grid is shown with a dashed line.

reflection coefficients, particularly for frequencies close to the Nyquist limit. Much earlier, a similar technique was applied to periodic solutions of Burgers' equation in one-dimension to increase the grid sampling near the steepest component of the wavefront [11], [12], [14]. A more comprehensive reference list of other applications is also given by Boyd [9]. Here, we explore the use of a mapped k-space pseudospectral method for time-domain simulations of propagating nonlinear waves where the density of grid points is increased in regions of the domain with steep variations in the wave field. In this correspondence, the analysis is restricted to simulations in one-dimension, which is sufficient to illustrate the merit of the approach. The implementation of the mapped pseudospectral method in higher dimensions is a simple extension of the one-dimensional case, however, the choice of optimal nonuniform grid mappings is more complex [15]. The extension to two and three spatial dimensions will be examined as part of future work.

B. The k-Space Pseudospectral Method

In most pseudospectral discretizations of time-dependent partial differential equations, solutions are obtained by iterating forward in time using a finite-difference approximation of the temporal gradients. The *k*-space pseudospectral method instead exploits the existence of an exact solution to the linearized wave equation for homogeneous media to improve the accuracy of the temporal discretization [8]. This allows larger time steps to be used for the same degree of accuracy. The *k*-space approach was recently applied to the discretization of coupled acoustic equations valid for modeling wave propagation through heterogeneous media, including cumulative nonlinear effects and power law acoustic absorption [6]. This approach is extended here to incorporate calculations on nonuniform grids using the mapped pseudospectral method.

The set of coupled first-order partial differential equations can be written as [6]

$$\frac{\partial \mathbf{u}}{\partial t} = -\frac{1}{\rho_0}\nabla p, \quad \frac{\partial \rho}{\partial t} = -(2\rho + \rho_0)\nabla \cdot \mathbf{u}, \qquad p = c_0^2\left(\rho + \frac{B}{2A}\frac{\rho^2}{\rho_0} - \mathrm{L}\rho\right). \tag{2}$$

Physically, these expressions correspond to momentum conservation, mass conservation, and an equation of state. Here, $\mathbf{u}$ is the acoustic particle velocity, p is the acoustic pressure, ρ is the acoustic density, c_0 and ρ_0 are the isentropic sound speed and ambient density in the medium, B/A is the nonlinearity parameter, and L is a power-law absorption operator dependent on the fractional Laplacian [16]. These equations are the first-order equivalents of a generalized Westervelt equation modified to include power law absorption [6].

Using the *k*-space pseudospectral method, the discrete form of these equations in one dimension for simulations on a nonuniform grid is given by

$$\begin{aligned}
\frac{\partial}{\partial x_\mathrm{n}} p^m &= \frac{\mathrm{d}x_\mathrm{u}}{\mathrm{d}x_\mathrm{n}} \mathbb{F}^{-1}\{ik_x\kappa\mathbb{F}\{p^m\}\}, \\
u^{m+1/2} &= u^{m-1/2} - \frac{\Delta t}{\rho_0}\frac{\partial}{\partial x_\mathrm{n}} p^m, \\
\frac{\partial}{\partial x_\mathrm{n}} u^{m+1/2} &= \frac{\mathrm{d}x_\mathrm{u}}{\mathrm{d}x_\mathrm{n}} \mathbb{F}^{-1}\{ik_x\kappa\mathbb{F}\{u^{m+1/2}\}\}, \\
\rho^{m+1} &= \frac{\rho^m - \Delta t\rho_0\frac{\partial}{\partial x_\mathrm{n}}u^{m+1/2}}{1 + 2\Delta t\frac{\partial}{\partial x_\mathrm{n}}u^{m+1/2}}, \\
p^{m+1} &= c_0^2\left(\rho^{m+1} + \frac{B}{2A}\frac{1}{\rho_0}(\rho^{m+1})^2 - \mathrm{L}\rho\right).
\end{aligned} \tag{3}$$

These expressions are equivalent to those given in [6], except for the two transformation gradients which map between uniform and nonuniform grids. The superscript m and $m + 1$ denote the function values at the current and next time points (including time staggering), the subscripts u and n denote uniform and nonuniform grids, Δt is the size of the time step, and κ is given by $\kappa = \mathrm{sinc}\,(c_\mathrm{ref}k\Delta t/2)$. The sinc term results from a nonstandard discretization of the time derivative that is known to reduce (or, in the case of suitably constrained material properties, eliminate) numerical dispersion [8].

These equations were implemented in Matlab (The MathWorks Inc., Natick, MA) as an extension to the open-source k-Wave Toolbox [17]. A perfectly matched layer was used to absorb the waves at the edges of the domain (this was applied on the nonuniform grid), and the grids were spatially and temporally staggered to improve accuracy [8]. Note that, when spatially staggered grids are used, the transformation gradient $\mathrm{d}x_\mathrm{u}/\mathrm{d}x_\mathrm{n}$ used to compute the spatial gradient of the particle velocity $\partial u/\partial x_\mathrm{n}$ must also be defined using the staggered grid points, i.e., using the uniform grid axis x_n shifted by half the grid point spacing $\Delta x_\mathrm{u}/2$.

III. Numerical Examples

A. Nonuniform Grid Optimization Using a Known Harmonic Distribution

To investigate the applicability of using nonuniform grids for modeling nonlinear ultrasound waves, we begin with a simple example. It is first assumed that an accurate reference solution is available from which a suitable nonuniform grid and transformation gradient can be derived (an example without this is discussed in the next section). In this case, the reference solution was computed using a uniform grid with 2048 grid points (including a perfectly matched layer with a thickness of 20 grid points on each side of the domain). The grid point spacing was set to 1.5 μm, supporting a maximum frequency of 50 MHz at two points per wavelength, and the time step was 3 ns, giving a Courant–Friedrichs–Lewy (CFL) number of 0.3, where CFL $= c_0\Delta t/\Delta x$. The medium parameters were set to be homogeneous, with $c_0 = 1500$ m·s^{-1}, $\rho_0 = 1000$ kg·m^{-3}, $B/A = 6$, and $\alpha_0 = 0.25$ dB·MHz^{-2}·cm^{-1}. The input signal was a 1-MHz sinusoid with an amplitude of 5 MPa injected as a mass source at the left-hand side of the domain. A snapshot of the pressure field after 25 μs is shown in Fig. 2(c).

To obtain a nonuniform grid mapping from the reference solution, the frequency spectrum of the steady-state time-varying pressure at each grid point was analyzed to determine the highest frequency harmonic contributing to the local waveform. This maximum was extracted by finding the highest frequency harmonic with an amplitude of more than 0.5% the amplitude of the fundamental frequency at that position. The variation in the maximum harmonic present in the local waveform with propagation distance is shown as the solid line in Fig. 2(a). This curve increases with distance due to the cumulative nature of the modeled nonlinear effects. The corresponding grid point spacing required to capture this frequency using two points per wavelength is shown as the solid line in Fig. 2(b). There is almost an order of magnitude difference in the grid spacing needed as the waveform steepens. When a uniform grid spacing is used, the discretization is globally constrained by the smallest grid point spacing required anywhere in the domain. In this case, this requires a computational grid with 580 grid points.

Given the variation in the required grid point spacing with distance, a nonuniform grid can then be derived. Here, an arctan/tan mapping was used, where [11], [12]

$$x_{\mathrm{n}} = \frac{2}{\pi}\tan^{-1}\left[\frac{1}{\beta}\tan\left(\frac{\pi}{2}(x_{\mathrm{u}}-1)\right)\right]+1. \quad (4)$$

This maps between normalized uniform grid points $x_{\mathrm{u}} \in [0,1]$ and nonuniform grid points $x_{\mathrm{n}} \in [0,1]$, where the parameter $\beta > 0$ controls the strength of the grid point clustering toward $x = 1$. The transformation gradient for this mapping is

$$\frac{\mathrm{d}x_{\mathrm{u}}}{\mathrm{d}x_{\mathrm{n}}} = \frac{\beta^2+1+(\beta^2-1)\cos(\pi x_{\mathrm{u}})}{2\beta}, \quad (5)$$

where $x_{\mathrm{u}} = 0, 1/N_x, 2/N_x, \ldots, 1 - 1/N_x$. The values for β and N_x were obtained by fitting (4) to the grid spacing data shown in Fig. 2(b) using unconstrained nonlinear minimization (fminsearch in Matlab). For this example, the obtained parameter values were $\beta = 1.7$ and $N_x = 366$ (the fitted curve is shown with a dashed line). Excluding the perfectly matched layer, this corresponds to a 40% reduction in the total number of grid points compared with using a uniform grid, which is significant. Using a CFL number of 0.05 to minimize any other sources of error, error norms calculated from the final pressure field using a nonuniform grid were $L_2 = 0.59\%$ and $L_\infty = 30$ kPa compared with $L_2 = 0.33\%$ and $L_\infty = 69$ kPa in the uniform case. (Here, the relative L_2 error norm is defined as $L_2 = \|p_{\mathrm{ref}}(x_i) - p(x_i)\|_2/\|p_{\mathrm{ref}}(x_i)\|_2$.) This confirms that the accuracy of the simulation is maintained.

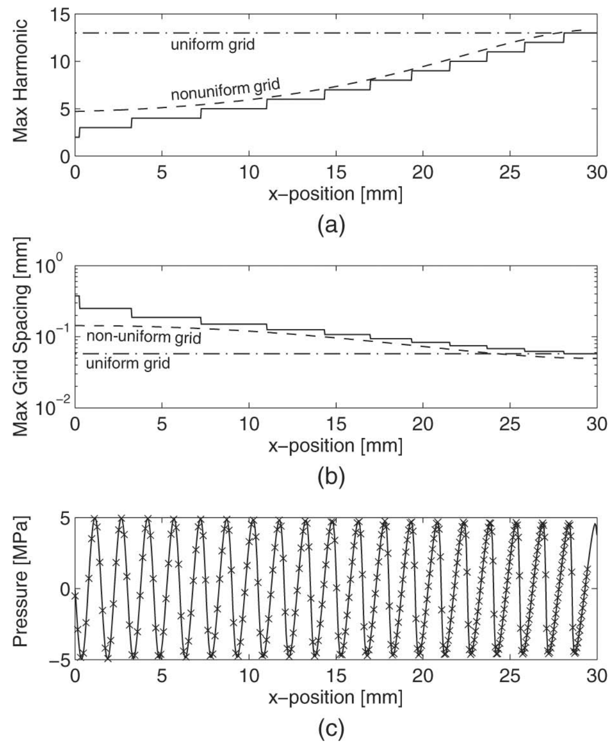

Fig. 2. Simulation of nonlinear wave propagation in 1-D. (a) Number of harmonics needed to accurately represent the waveform at each position (solid line), maximum harmonic supported by the grid at each position using a uniform grid (dash dot line), and maximum harmonic supported by the grid at each position using an optimized nonuniform grid (dashed line). (b) Analogous information for the maximum grid spacing at each grid position. (c) Snapshot of the pressure within the domain using a uniform grid (solid line) and an optimized nonuniform grid (crosses). The nonuniform grid retains the accuracy of the simulation with a 40% reduction in grid points.

B. Nonuniform Grid Optimization Using Envelope-Based Equidistribution

Although the example provided in the previous section illustrates the potential benefits of using a nonuniform grid for simulating nonlinear ultrasound waves, in many cases an accurate reference solution will not be available *a priori*. However, if some basic information about the wave field is still available (for example, from a simulation on a coarse uniform grid), this can similarly be used to derive an appropriate nonuniform grid mapping. In this case, rather than analyzing the time history of the wave field at each grid point, a monitor function is constructed from a snapshot of the wave field at a particular time. The monitor function assesses the variation of the pressure field between each pair of adjacent grid points. A more suitable distribution of grid points can then be estimated based on the concept of equidistribution [15]. This works by shuffling the grid points such that the changes in the field values are roughly equally distributed between the grid points.

In the case of nonlinear wave propagation, the wave field may be complex, with large variations between the grid points that oscillate in time. However, for a continuous wave source in steady state, the overall spatial distribution of energy at higher frequency harmonics (which dictates the required grid spacing) will remain constant. A suitable nonuniform grid can thus be derived by constructing a monitor function that depends only on the overall *envelope* of the variations in the wave field, rather than variations on a small scale. This is illustrated in Fig. 3. Here, the monitor function was created from the pressure field after 25 μs using the uniform simulation with $N_x = 580$ discussed in the previous section. The magnitude of the pressure variation between each of the grid points is shown in Fig. 3(a). The steeper peaks correspond to sharper variations in the wave field (in this case, resulting from nonlinearity). The exact position of these peaks will migrate with time, however, the overall envelope will remain approximately constant. In this case, the monitor

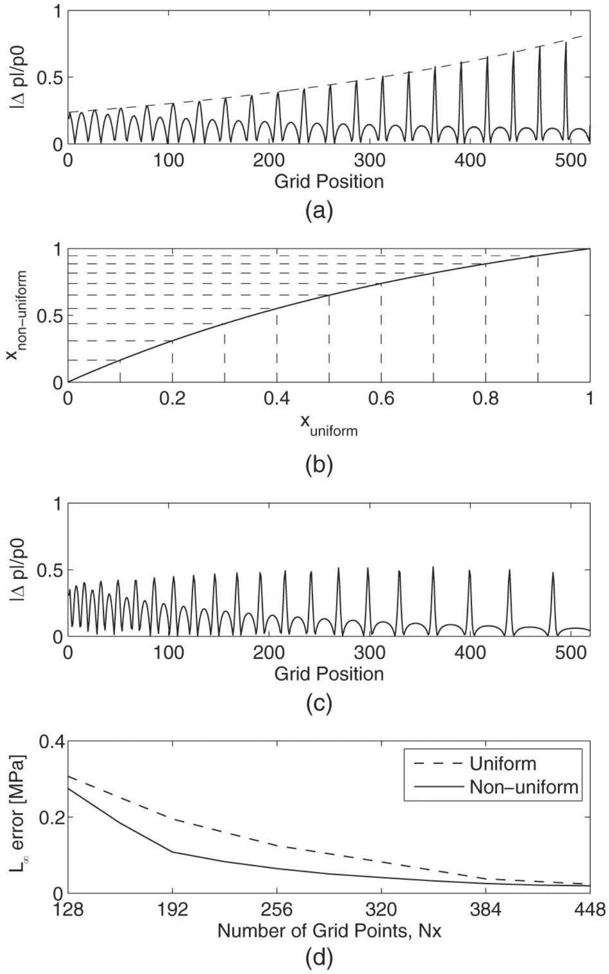

Fig. 3. Deriving an optimized nonuniform grid for a 1-D simulation using envelope-based equidistribution. (a) Magnitude of the pressure variation between pairs of adjacent grid points (solid line) and an exponential function fitted to the envelope (dashed line). (b) Nonuniform grid mapping derived from the envelope. (c) Magnitude of the pressure variation between grid points using the nonuniform grid. The sizes of the peaks are now approximately equal across the grid. (d) Variation in the L_∞ error norm with the number of grid points using a uniform grid (dashed line) and nonuniform grid derived using equidistribution (solid line).

function was constructed by fitting an exponential function of the form $x_{\text{fit}} = ae^{bx_{\text{u}}}$ to the peaks shown in Fig. 3(a). The fitted exponential is shown with the dashed line.

Once the monitor function is known, the nonuniform grid points x_n can be extracted in three steps as follows: 1) take the reciprocal of the monitor function values; 2) calculate the cumulative sum (e.g., using cumsum in Matlab); and 3) normalize the result between 0 and 1. For an exponential monitor function, the nonuniform grid mapping is given by

$$x_{\text{n}} = \frac{1 - e^{-bx_{\text{u}}}}{1 - e^{-b}}, \tag{6}$$

where $x_{\text{u}}, x_{\text{n}} \in [0,1]$ and a and b are the exponential parameters obtained from the fitting procedure. The corresponding transformation gradient is given by

$$\frac{\mathrm{d}x_{\text{u}}}{\mathrm{d}x_{\text{n}}} = \frac{1 - e^{-b}}{be^{-bx_{\text{u}}}}. \tag{7}$$

The nonuniform grid mapping derived in this fashion for the monitor function given in Fig. 3(a) is shown in Fig. 3(b). The corresponding magnitude of the pressure variation between each pair of adjacent grid points derived from a simulation using the nonuniform grid is given in Fig. 3(c). The envelope of this variation is now approximately flat across the domain. This improves the accuracy of the simulation, particularly in regions where the wave field varies rapidly. The variation in the L_∞ error norm with the number of grid points used is shown in Fig. 3(d). In each case, a uniform simulation with the same number of grid points was performed first. This was then used to derive a suitable nonuniform grid using envelope-based equidistribution. The use of the nonuniform grid gives a noticeable improvement in the accuracy of the simulation. The total simulation time using uniform and nonuniform grids in each case were within 3%, which illustrates the computational efficiency of the technique.

IV. Conclusion and Discussion

A mapped k-space pseudospectral method for simulating the propagation of nonlinear waves on nonuniform computational grids has been described. This allows the grid points to be clustered around regions of the wave field that are sharply varying, which improves accuracy. Two methods for selecting the nonuniform grid mapping have also been presented. The first is based on extracting the highest frequency that contributes to the local waveform using an accurate reference simulation. This is then used to define the required grid point spacing and hence the location of the nonuniform grid points. The second method is based on equidistribution, in which the grid points are shuffled so that the envelope of the variation in the pressure field between grid points is approximately constant across the domain. In both cases, using a nonuniform grid significantly reduces the number of grid points required for accurate simulations. Equivalently, for a fixed number of grid points, using a nonuniform grid gives a noticeable improvement in accuracy. This illustrates the utility of using nonuniform grids for modeling nonlinear acoustic waves. Future work will address extending this to two and three spatial dimensions as well as the use of adaptive procedures to update the mesh during the simulation [15].

Acknowledgments

The author thanks J. Jaros for useful discussion on the efficient implementation of Fourier pseudospectral methods, and B. Cox for providing comments on the manuscript.

References

[1] J. Huijssen and M. D. Verweij, "An iterative method for the computation of nonlinear, wide-angle, pulsed acoustic fields of medical diagnostic transducers," *J. Acoust. Soc. Am.*, vol. 127, no. 1, pp. 33–44, 2010.

[2] P. V. Yuldashev and V. A. Khokhlova, "Simulation of three-dimensional nonlinear fields of ultrasound therapeutic arrays," *Acoust. Phys.*, vol. 57, no. 3, pp. 334–343, 2011.

[3] V. A. Khokhlova, O. V. Bessonova, J. E. Soneson, M. S. Canney, M. R. Bailey, and L. A. Crum, "Bandwidth limitations in characterization of high intensity focused ultrasound fields in the presence of shocks," in *9th Int. Symp. Therapeutic Ultrasound*, 2010, pp. 363–366.

[4] D. W. Zingg, "Comparison of high-accuracy finite-difference methods for linear wave propagation," *SIAM J. Sci. Comput.*, vol. 22, no. 2, pp. 476–502, 2000.

[5] G. Wojcik, J. Mould, S. Ayter, and L. Carcione, "A study of second harmonic generation by focused medical transducer pulses," in *Proc. IEEE Ultrasonics Symp.*, 1998, pp. 1583–1588.

[6] B. E. Treeby, J. Jaros, A. P. Rendell, and B. T. Cox, "Modeling nonlinear ultrasound propagation in heterogeneous media with power law absorption using a *k*-space pseudospectral method," *J. Acoust. Soc. Am.*, vol. 131, no. 6, pp. 4324–4336, 2012.

[7] Y. Jing, T. Wang, and G. T. Clement, "A *k*-space method for moderately nonlinear wave propagation," *IEEE Trans. Ultrason. Ferroelectr. Freq. Control*, vol. 59, no. 8, pp. 1664–1673, 2012.

[8] M. Tabei, T. D. Mast, and R. C. Waag, "A *k*-space method for coupled first-order acoustic propagation equations," *J. Acoust. Soc. Am.*, vol. 111, no. 1, pt. 1, pp. 53–63, 2002.

[9] J. P. Boyd, *Chebyshev and Fourier Spectral Methods*. Mineola, NY: Dover Publications, 2001.

[10] J. Lu, J. Pan, and B. Xu, "Time-domain calculation of acoustical wave propagation in discontinuous media using acoustical wave propagator with mapped pseudospectral method," *J. Acoust. Soc. Am.*, vol. 118, no. 6, pp. 3408–3419, 2005.

[11] J. M. Augenbaum, "An adaptive pseudospectral method for discontinuous problems," *Appl. Numer. Math.*, vol. 5, no. 6, pp. 459–480, 1989.

[12] J. P. Boyd, "The arctan/tan and Kepler-Burgers mappings for periodic solutions with a shock, front, or internal boundary layer," *J. Comput. Phys.*, vol. 98, no. 2, pp. 181–193, 1992.

[13] X. Gao, M. Mirotznik, and S. Shi, "Applying a mapped pseudospectral time-domain method in simulating diffractive optical elements," *J. Opt. Soc. Am. A*, vol. 21, no. 5, pp. 777–785, 2004.

[14] H. Guillard and R. Peyret, "On the use of spectral methods for the numerical solution of stiff problems," *Comput. Methods Appl. Mech. Eng.*, vol. 66, no. 1, pp. 17–43, 1988.

[15] W. Huang and R. D. Russell, *Adaptive Moving Mesh Methods*. New York: Springer, 2011.

[16] B. E. Treeby and B. T. Cox, "Modeling power law absorption and dispersion for acoustic propagation using the fractional Laplacian," *J. Acoust. Soc. Am.*, vol. 127, no. 5, pp. 2741–2748, 2010.

[17] B. E. Treeby and B. T. Cox, "k-Wave: MATLAB toolbox for the simulation and reconstruction of photoacoustic wave fields," *J. Biomed. Opt.*, vol. 15, no. 2, p. 021314 2010.